

POTENTIAL AND LIMITATIONS FOR HYDRONIC RADIANT SLABS USING WATERSIDE FREE COOLING AND DEDICATED OUTSIDE AIR SYSTEMS

Timothy Moore

Center for the Built Environment (CBE), University of California, Berkeley, CA
tmoore@whole-systems-design.com

ABSTRACT

This paper investigates the potential and limitations for slab-integrated radiant cooling using an indirect-evaporative fluid cooler as the primary source of cooling supply water. The analysis focuses on cooling capacity and energy consumption, while maintaining thermal comfort criteria, in comparison to an appropriately optimized all-air VAV system. Modeling of radiant cooling using Integrated Environmental Solution's Virtual Environment (iesVE) allowed for simulation of directly coupled thermal mass, controlled surface temperatures, and radiant exchange between surfaces. The model also accounts for hydronic tubing size, material, and spacing; density and depth of concrete; convective heat transfer coefficients specific to the chilled surfaces; thermal stratification in the conditioned space; a dedicated outside air system with indirect evaporative cooling; and an evaporative fluid cooler as the primary source of cooling supply water.

INTRODUCTION

Numerous studies have described potential energy savings and comfort characteristics associated with hydronic radiant cooling, and some have compared this type of system with others. However, there appears still to be considerable lack of clarity regarding how slab-integrated hydronic radiant cooling compares to a well-optimized modern all-air system. Furthermore, there appears to be a general lack of information as to how practitioners in the field might best make a fair and appropriately comprehensive comparison between such systems using tools and methods that are well suited both to the simulation task and the context of a typical commercial building project. This paper attempts to address these issues first by describing repeatable methods for this comparison using one available analytical tool with a suitably practical interface and appropriately detailed modeling capabilities. Simulation results reported here are intended shed light on both the characteristics of the systems compared and the nature of what can be gleaned from the methods employed.

METHODS AND ASSUMPTIONS

Radiant cooling and all-air systems, as described below, are compared in the context of a simple five-story office building with typical loads and very modest optimization of the building shell.

The climate selected for this study is Denver, Colorado. The significant seasonal and diurnal variation within this climate offer an opportunity to compare how each of the two systems handles fluctuations in load and load diversity with respect to core vs. perimeter thermal zones. It is also a suitably dry climate for application of a hydronic cooling system using only an evaporative fluid cooler (close-circuit cooling tower) as the cooling water source. This study is concerned primarily with cooling performance, including associated reheat when zone cooling demands differ; thus the simulation runs are for the just the months of May through September.

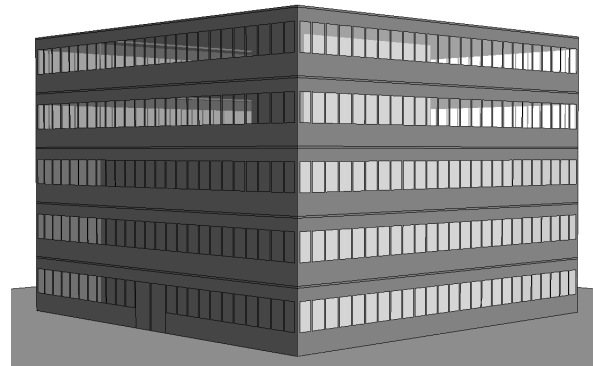


Figure 1: Exterior view of office building as modeled

The fair comparison of very different systems and the development of methods readily applicable to other projects suggested a notably generic building: Good insulation, tight construction, high-performance glazing, and a high-albedo roof are included. The building is otherwise relatively sub-optimal in some respects. For example, the floor plate is fairly deep, there are no physical shading devices, and there are no daylighting or occupancy controls for electric lighting.

The total floor area of the building is 3,125 m² (33,637 ft²). The 19 × 19-m (62 × 62-ft) interior zone and entire 25 × 25-m (82 × 82-ft) floor plate on the top two floors are open-plan, with the exception of a partitioned conference room and a 5 × 5-m (16.4 × 16.4-ft) concrete core with shear walls housing an elevator, stair well, electrical, janitorial closet, and restrooms. However, as can be seen in Figure 1, the perimeter zones on the first three floors are partitioned off via uninsulated gypsum-board interior walls at a depth of 3 meters (10 ft) from the façade. This provides means of studying the behavior of the HVAC systems with respect to variation in perimeter loads with orientation.

Common building elements

The building construction, internal loads, schedules, ventilation requirements, and a zone-level exhaust fans common to both simulation runs are as follows:

- Floor decks: All floor decks, including the ground floor and roof deck, are constructed of 200-mm (8-in) cast concrete slabs. While central to the hydronic cooling scheme, the common application of this construction also affords the all-air system some benefit in terms of the exposed interior thermal mass buffering midday cooling loads. All floors are covered with synthetic carpet and pad.
 - Foundation: The 200-mm (8-in) concrete slab-on-grade ground floor is insulated, for both schemes, with continuous 50-mm (2-in) polyisocyanurate to a U-value of 0.44 W/m²-K (R-13 h-ft²-°F/Btu). This construction sits on a 50-mm (2-in) layer of gravel and 500-mm (~20-in) of soil, for which thermal properties are included in the model. Adjacent ground temperatures are reset monthly via a schedule of TMY-2 ground temperature data.
 - Concrete core: An interior shear-wall core houses stairwells, elevators, and other services, and is constructed of 150-mm (6-in) uninsulated cast concrete and directly coupled to all floor slabs.
 - Roof: The roof assembly—on top of the reinforced concrete roof deck with embedded hydronic tubing—includes a highly reflective white TPO membrane (initial solar reflectance of 0.85, modeled as 0.30, assuming significant degradation from soiling) and continuous rigid EPS foam insulation. The roofing assembly U-value is 0.19 W/m²-K (R-30 h-ft²-°F/Btu).
 - Walls: Exterior walls comprise steel-stud framing with gypsum board interior finish, fiberglass batt insulation between the studs, and continuous rigid foam insulating board behind sheet-metal exterior cladding. The U-value for the complete assembly is 0.26 W/m²-K (R-Value of 22 hr-ft²-°F/Btu).
 - Glazing: The glazed area, including mullions, is 40% of the complete exterior floor-to-floor façade area for all orientations (slightly more where glass doors are included on the north and south ground-floor facades). Glazing units using PPG Caribia SolarCool-coated exterior glass and SolaBan-60 low-e coated clear interior glass, assembled in Lawrence Berkeley National Lab's Window5, have solar heat-gain coefficient (SHGC) of 0.14, visible transmittance of 21%, and center-of-glass U-value of 1.64 W/m²-K (0.29 Btu/ hr-ft²-°F). The window assembly U-factor, including thermally broken aluminum mullions, is 2.1 W/m²-K (0.37 Btu/ hr-ft²-°F). No exterior shading devices are included and, given their limited benefit and potential for remaining open, no interior blinds are modeled.
 - Infiltration and exfiltration: Infiltration is assumed to be 0.1 ACH for all perimeter zones, given moderately tight construction. This equates to 0.94 l/s-m² (0.02 cfm/ft²) in those zones. Exfiltration is driven by building pressurization via supply air fan and is thus modeled within the HVAC network as a path from the rooms and return air to the outdoor environment. It is controlled to vary with the supply fan airflow volume from a minimum of 195 l/s (413 cfm) to a maximum of 650 l/s (1,377 cfm) for the entire building. This equates to 0.07 to 0.23 ACH at the minimum and maximum supply fan airflow, respectively.
- The simulation tool employed has the capability to model infiltration and exfiltration as a function of weather file wind speed and direction and assigned crack areas and exposure factors for all constructions and fenestration. However, this requires somewhat longer simulation run times and was deemed unnecessary for the present study.
- Equipment: The equipment load density is 8 W/m² (0.75 W/ft²). The equipment is assumed to have a radiant heat fraction of 20%, and otherwise contributes to space loads only through convective heat transfer. The schedule for this load is at least 50% 8:00–9:00 AM, ramping to 100% from 9:00 AM until 5:00 PM, then down to 50% again 5:00–6:00 PM. There is a minimum 10% plug load at all times, including nights, weekends, and holidays.
 - Lighting: The electric lighting power density (LPD) is 8 W/m² (0.75 W/ft²), and is assumed to be 45% radiant and 55% convective. The lighting schedule is identical to the equipment schedule.

- Occupants: Peak occupancy is 225 people (45 per floor). The net occupied space per person is 14 m² (150 ft²). At the gross whole-building level, this is 18.6 m² (200 ft²) per person. The occupancy schedule is 50% minimum for all hours from 8:00 AM to 6:00 PM, ramping up to 100% for the morning hours of 9:00–12:00 and again for afternoon hours of 2:00–5:00 PM. Occupant heat gains are 90 W (307 Btu/hr) per person sensible and 60 W (205 Btu/hr) per person latent. Sensible gain is split evenly between radiant and convective components; however, the convective would tend to dominate in an air-cooled environment, where surfaces are warmer, and the radiant component would tend to dominate with cooled surfaces.
- Ventilation: Minimum outside-air ventilation at the zone level is 10.0 l/s (21.2 cfm) per person at peak occupancy and 0.78 l/s-m² (0.15 cfm/ft²).
- Exhaust fans: Because each is assumed to have similar efficiency, static pressure, and schedule, exhaust fans for rest rooms, copy rooms, etc. are included in the HVAC airside network as a single constant-volume fan and path to the outside.
- Domestic hot water: Because only HVAC energy is tracked in this study, and domestic hot water does not make a significant indirect contribution to HVAC loads, domestic hot water is not modeled.

HVAC Systems

There will always be room for asking how the outcome of this comparison might have been different if, for example, the baseline were a dual-duct, dual-fan system. However, there is value in *first* comparing to a well-understood baseline that represents best practice for the size and type of system and building. The baseline system is thus an attempt at fair representation of a common configuration for mid-sized office buildings. This “plain vanilla” system is meant to be familiar and yet relatively well optimized in terms of equipment, features, and controls. An alternate version of the same

all-air system, including a waterside economizer or waterside “free cooling” (WSFC) is modeled as well.

VAV re-heat with economizer and cooling coil reset

The baseline for comparison is an all-air variable-air-volume (VAV) system with terminal re-heat, outside-air economizer, and cooling supply air temperature reset.

A water-cooled chiller with screw type compressor of relatively high performance (less than 0.6 kW/ton from 40 to 75% of maximum load) is modeled with load-dependant COPs. The 117-kW (33-ton) chiller is sized to 15% over the cooling design day load. The combined part-load COPs for the chiller plus chilled-water pump, condenser-water pump, and cooling tower at 20, 40, 60, 80, and 100% load and ARI standard operating conditions are 3.7, 4.4, 4.7, 4.3, and 3.9, respectively.

Hot water heating at the air handler and terminal re-heat are provided by a high-efficiency condensing boiler that continuously modulates its output, efficiently meeting the current load by maintaining a set return water temperature. The 90-kW (307-kBtu) boiler is sized to 25% over the heating design day peak load. At a return water temperature of 54.5°C (130°F), boiler efficiencies for 25, 45, 65, 80, and 100% load are 93, 92.5, 92, 91.5, and 91%, respectively.

Supply fans are variable from 2,800 l/s (5,933 cfm) to 8,320 l/s (17,622 cfm), with total static pressure of 350 Pa (1.4 i.w.c.). Return fans are variable from 2,190 l/s (4,640 cfm) to 7,250 l/s (15,362 cfm), with total static pressure of 250 Pa (1.0 i.w.c.). Both are modeled with performance based on backward-curved centrifugal fans (peak fan efficiency of 80%) and premium efficiency motors with variable-speed drives (combined fan plus motor operating efficiency ranging from 70 to 75%).

The minimum flow for the outside air economizer is equal to the required minimum ventilation, its maximum flow is equal to the supply fan capacity, and its damper set is controlled to deliver a mixed-air temperature that varies inversely in proportion to the return-air

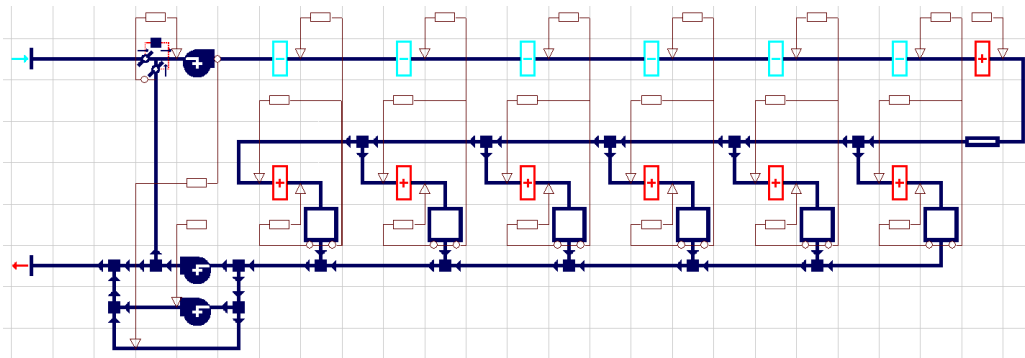
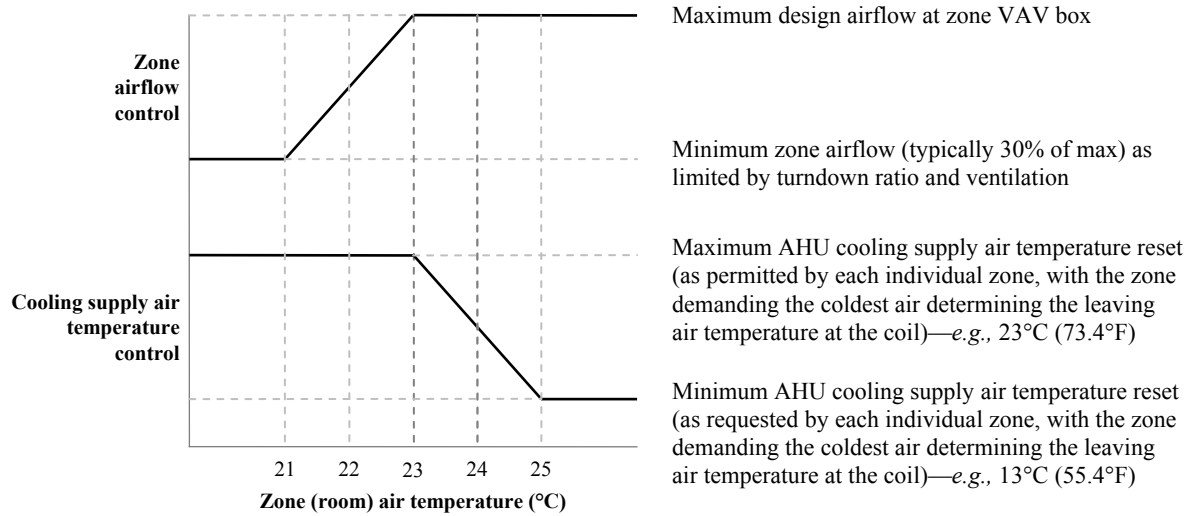


Figure 2: Baseline VAV system (airside and controls network for just one floor is shown)



Zone cooling control midband is effectively 23°C. When loads require cooler supply air, zone temperatures tend toward 24°C reset midband

Figure 3: Control sequence for zone airflow and AHU cooling coil leaving air temperature reset

temperature. This provides mixed-air temperature reset that takes full advantage of airside free cooling while minimizing mechanical cooling of outside air.

The waterside economizer or “free cooling” (WSFC) for the second VAV scenario is based upon an available tower somewhat larger than needed just to reject heat from the fully loaded chiller. Supply water temperature, however, is constrained by the 2.2 K (4°F) approach. Thus, while the tower has ample capacity when outdoor wet-bulb temperatures reach 23°C (73.4°F) and entering water from the coils is just a few degrees warmer, the supply-air temperature, as reset to meet zone demand, may require colder water than the tower can provide. WSFC thus runs when it can meet the cooling coil load, and, when it can’t, hands off to the water-cooled chiller.

Supply air ducts passing through the interior zone are insulated to a U-value of 1.3 W/m²-K (R-value of 4.4 h-ft²-°F/Btu) with continuous 25-mm (1-in) rigid polymer-coated fiberglass duct-liner. The surface area of the supply ducts subject to heat gain is 80 m² (~861 ft²) per floor, or 400 m² (~4,304 ft²) for the complete building.

Supply air temperature reset—continuous adjustment of the coil leaving air temperature (LAT)—from 13°C (55.4°F) up to the room-air cooling midband eliminates unnecessary reheat and permits this system to take full advantage of airside *and* waterside economizer hours.

Cooling supply air temperature reset is modeled and controlled as shown in Figures 2 and 3: A single cooling coil at the air handler is modeled as series string of coils, each associated with a separate zone. The composite LAT for the series is thus forced to equal that

required by the zone demanding the lowest cooling air temperature at any given time step (once zone airflow has been adjusted up to the VAV-box maximum). This correctly models cooling supply air temperature reset with this particular simulation tool. Successful reset to maximize economizer hours and operational efficiency of the chiller also requires airflow to interior zones to be sized to permit use of the maximum cooling reset temperature. The airflow-first control sequence used (Figure 3) is a common reset strategy. Swapping the midband temperatures for the airflow and cooling controllers—a cooling-reset-first sequence—had higher energy consumption, and thus was not used.

Both because the Denver climate is very dry, and thus there is no significant need for dehumidification, and because dehumidification for the DOAS would involve a desiccant wheel that presently requires a complex workaround within this particular simulation tool, a humidity sensor and control signal are not modeled within the cooling coil LAT reset control. For the VAV system, this permits supply air temperatures based upon sensible cooling demand only, further extending the number of air- and waterside economizers hours.

Loops around the RA path and return fan (Figure 2) appropriately reduce the return airflow in keeping with zone-level exhaust fans and exfiltration. Constant-volume exhaust fans and associated static pressure for restrooms, copy rooms, etc. are combined as a single fan and airflow path. Exfiltration based on construction tightness and building pressurization has a separate path with no fan and airflow proportional to OA flow rate.

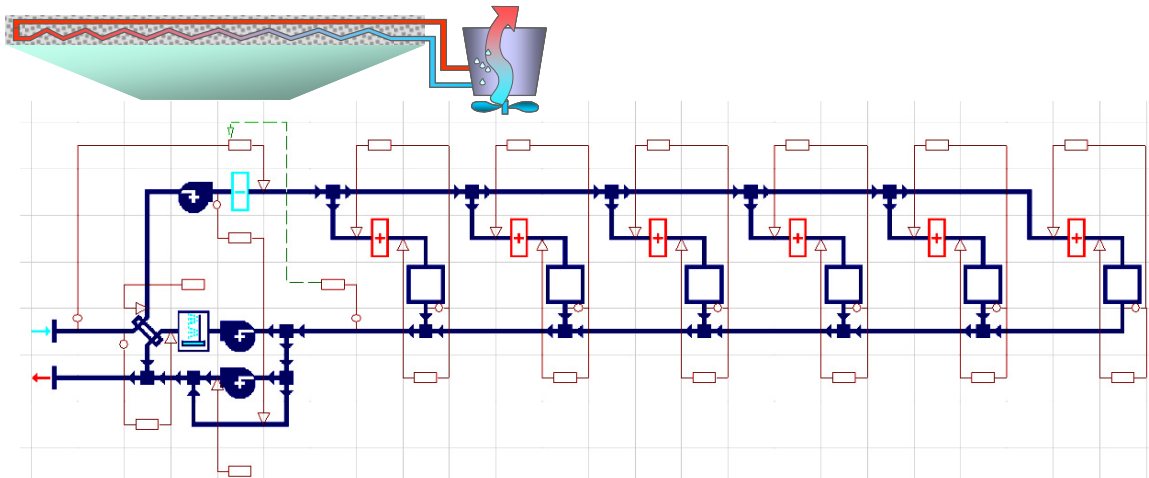


Figure 4: Conceptual illustration and schematic of the radiant cooling plus DOAS (airside and controls network for just one floor is shown)

Hydronic radiant cooling and heating with evaporative cooling water source and DOAS

The hydronic radiant cooling slabs are modeled as fully geometric building elements—*i.e.*, with thermal mass, direct absorption of incident solar gain, direct radiant exchange between surfaces, and appropriate convective heat transfer coefficients for the surface-to-air delta-T.

A conceptual illustration (top of Figure 4) emphasizes direct coupling of radiant slabs to the closed-circuit cooling tower without the use of a chiller. The airside schematic below it shows the DOAS with indirect evaporative cooling and energy recovery. The cooling coil on this airside portion of the system also uses the cooling tower as its chilled water source.

The overhead hydronic radiant cooling slab is the primary means by which this system addresses sensible loads in the space. Peak radiant slab cooling capacity as simulated was 62.5 W/m^2 (5.8 W/ft^2) as augmented by 12.0 W/m^2 (1.1 W/ft^2) coincident cooling from the DOAS, for a total of 74.6 W/m^2 (6.9 W/ft^2). The chilled slab, hydronic system, and cooling-tower source of cooling supply water are described below.

The dedicated outside air system (DOAS) has both indirect evaporative cooling with an integral energy recovery heat exchanger and a cooling coil served by the cooling tower. Supply airflow with 100% outside air is variable from the design minimum outside-air volume of 2,250 l/s (4,770 cfm) up to 3,250 l/s (6,900 cfm). At the low end, this equates to 10 l/s (21.2 cfm) per person and 0.78 l/s-m^2 (0.15 cfm/ft^2). For this system, a minimum supply airflow equal to the sum of zone design minimum ventilation requirements is permitted by the lack of any recirculation, thus ensuring that all zones will receive at least the design minimum OA.

Given the absence of VAV boxes and reduced face velocity resulting from reduced airflow over the same cooling coil and heat-exchanger face area, total static pressure is 250 Pa (1.0 i.w.c.) at supply fan and return fans. Both are modeled with performance based on backward-curved centrifugal fans (peak fan efficiency of 80%) and premium efficiency motors with variable-speed drives (combined fan plus motor operating efficiency ranging from 70 to 75%).

Supply air ducts pass through the interior zones, as in the baseline VAV system; however, the surface area of the ductwork is reduced 43.4% in keeping with the smaller ducts afforded by 68% lower maximum airflow.

Exfiltration, as driven by building pressurization, varies from 130 l/s (270 cfm) to 210 l/s (440 cfm) with OA airflow. At its maximum, this is 32% of the maximum exfiltration for the baseline all-air system.

Chilled building components and surfaces

Chilled slabs are modeled as separate thermal zones. Hydronic tubing is equidistant—at 100 mm (4 in)—from top and bottom surfaces. With the exception of the slab-on-grade ground floor (insulated as described above under Common Building Elements), both slab surfaces are thermally active. Ceiling surfaces are exposed and floor surfaces are carpeted.

The internal volume of the slab zone was minimized to just 0.1 l/m^2 ($0.57 \text{ in}^3/\text{ft}^2$) floor area, or an internal height of just 0.1 mm (0.004 in), as means of essentially eliminating the air volume without having a volume of zero. The hydronic Chilled Ceiling component provided within Virtual Environment, which amounts to a controllable hydronic loop with thermal capacity, flow, mass, and pump power was then located within the minimized volume of the chilled slab thermal zone. The

thermal capacity of this hydronic cooling component was then set to be 100% convective to force its interaction with the slab materials to be similar to that of the water inside of the hydronic cooling loop.

The slabs are concrete at 2100 kg/m³ (131 lb/ft³) and a specific heat capacity of 840 J/kg-K (0.2 Btu/lb-°F). The conductivity of the concrete has been adjusted from 1.40 W/m-K down to 1.10 and 1.14 W/m-K for the interior and perimeter zone slabs, respectively, to account for the size, material, and spacing of the hydronic tubing. The difference between the interior and perimeter slabs is a function of the tube diameter. This adjustment was made using an approximate solution to Laplace's equation in the slab (Gough 2007). Air-film resistance and emissivity for the inside surfaces of the slab zones were set to values approaching zero and 1.0, respectively, as zero values are not permitted and these surfaces need to be represented as if they are in direct contact with the cooling water.

As a check of appropriate cooling capacity per supply water temperature, flow rate, and surface-to-air delta-T, the bottom portion of the slab was replaced with a sheet of aluminum, the top was replaced with insulating foam, and loads were held constant. This configuration had cooling capacity closely matching typical manufacturer specifications over a range of input parameters.

Flow velocity per modeled water flow, tube diameter, and number of loops was used to determine equivalent pipe-length for valves, headers, etc. Friction head loss calculated with the Hazen-Williams roughness constant for polymer tubing resulted in circulation pump power of 37 W/l-s (2.4 W/gpm) and 47 W/l-s (3.0 W/gpm) for interior and perimeter zone hydronic circuits, respectively.

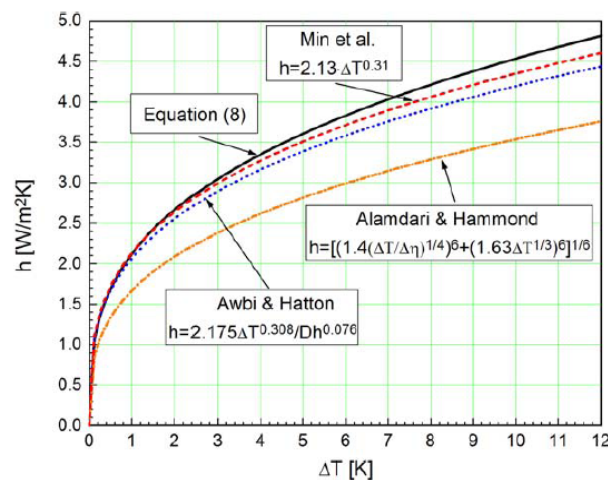


Figure 5: Results from Novoselac et al. (2006) showing convective heat transfer correlations for chilled overhead surfaces (Equation 8) developed in a controlled laboratory test chamber.

Natural convection at actively cooled surfaces

Previously established variable heat transfer coefficients for natural convection, including those from Alamdari & Hammond (1983), Awbi & Hatton (2000), and CIBSE, appear poorly suited to modeling chilled ceiling surfaces. Correlations—“Equation (8)” in Figure 5—developed in laboratory experiments by Novoselac et al. (2006) indicate higher rates of convective heat transfer for chilled surfaces, and thus greater cooling capacity than would be predicted using each of the other coefficients noted. The newly developed convective heat transfer coefficient for chilled overhead surfaces yields an increase of approximately 5–6% in cooling capacity for the chilled slab modeled as compared to using the Alamdari & Hammond variable coefficient. For the CIBSE variable coefficient, cooling capacity appears to be under-predicted by approximately 3–4%. Although it was not possible to introduce it as a variable coefficient within the simulation tool used for this study, the difference with the Awbi & Hatton coefficient should be on the order of one third of CIBSE result. In all cases, differences in predicted capacity depend upon the surface-to-air delta-T and the relative mix of convective and radiant heat sources in the space. In the case of the CIBSE variable coefficient, the predicted result also depends upon mean air velocity in the space and how this is reflected in the model.

The new coefficient from Novoselac et al. was used for just the downward facing surface of the chilled slab as modeled for this report.

$$h_c = 2.12 \times \Delta T^{0.33} \text{ W/m}^2\text{-K}$$

$$(h_c = 0.308 \times \Delta T^{0.33} \text{ Btu/h} \times \text{ft}^2 \times \text{°F})$$

Where: h_c = convective heat transfer coefficient
 ΔT = surface-to-air temperature difference in K (°F)

Cooling Tower

The supply water source for the hydronic slabs and cooling coils is a closed-circuit cooling tower with 2.2 K (4°F) approach. A simplified model of cooling tower operation maintains supply water temperature for the hydronic radiant slab and DOAS cooling coil in keeping with cooling tower approach and hourly outdoor wet-bulb temperatures in the TMY weather file. Based upon performance for an actual available cooling tower, this simplified model provides 15 to 19 kW cooling per kW electric input (i.e., consuming 0.24–0.18 kW_e/ton cooling), including tower fan, make-up water pump, and primary chilled-water (CHW) loop circulation pump (i.e., excluding only zone circulation pumps). This is modeled as a chilled water source with fixed approach to the varying outdoor wet-bulb temperature and a

coefficient of performance (COP) varying from 15 to 19 at outdoor WBTs of 60.8 to 10°C (50°F), respectively. Actual COP and approach also vary with the entering water temperature according to part-load conditions. Thus tower energy consumption for this simplified model is an approximation of actual performance.

RESULTS AND DISCUSSION

Simulated cooling system energy consumption for May through September (Table 1 and Figure 8) suggests that there is considerable potential for energy savings with radiant cooling in climates suited to evaporative cooling of supply water via a cooling tower. An alternate VAV system scenario with waterside economizer or waterside “free cooling” (WSFC) demonstrates the extent to which the baseline VAV system could capture a portion of the same benefit from the use of its cooling tower as cooling supply water source when conditions permit. In all cases, WSFC still uses fan and pump energy.

Peak radiant slab cooling capacity, as simulated within the top-floor west perimeter zone, was 62.5 W/m² (5.8 W/ft²). This was augmented by 12.0 W/m² (1.1 W/ft²) coincident cooling from the DOAS, for a total of 74.6 Wm² (6.9 W/ft²) peak sensible cooling.

The combination of evaporative cooling and nighttime precooling opportunities, system efficacies, and thermal inertia of the slab-integrated hydronic cooling system reduced the seasonal peak cooling system power by 61% relative to the baseline all-air VAV system and 34% relative to the all-air VAV system with WSFC.

Both systems were capable of controlling interior air temperature consistently below 25°C (77°F) for all hours of the May through September cooling season. However, because the all-air system must cool surfaces via convective heat transfer; all interior surfaces tend to be warmer than the air during cooling operation. When there is significant incident solar radiation striking the window glazing, the mean radiant temperature (MRT) in the spaces conditioned by the all-air system tends thus to be considerably more elevated than for the same set of surfaces in the spaces conditioned by the radiant cooling system. Figure 6 shows number of May through September hours for which the operative or dry resultant temperature—accounting for both air and

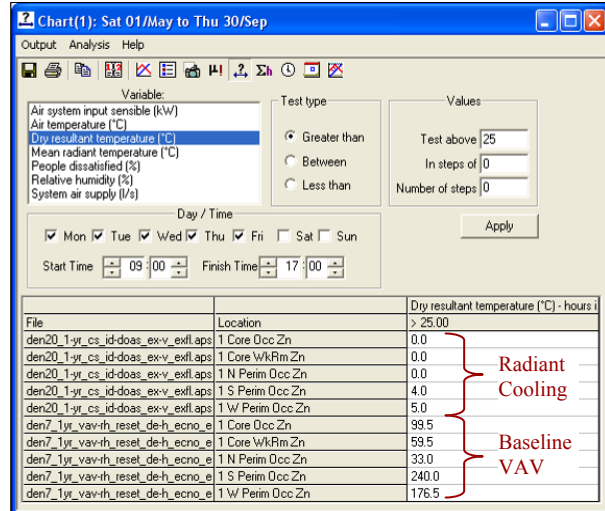


Figure 6: Comparison of May through September hours within the conditioned spaces that exceeded 25°C dry resultant (vs. dry-bulb) temperature

mean radiant temperatures—is elevated above 25°C (77°F). These results suggest that the simulated radiant cooling capacity and control strategy exceed the goal of ensuring comparable performance. Furthermore, they suggest that radiant cooling may provide improved comfort in certain perimeter-zone environments.

Comfort results for the radiant cooling indicated maintenance of percent people dissatisfied (PPD) below 10% as required to meet requirements of ASHRAE Standard 55-2004 thermal comfort for all regularly occupied hours in May through September. This was determined with a 75 W occupant activity level (equivalent to a 70-kg person performing sedentary office work at a metabolic rate of 1.0 Met) and minimal monthly adjustment of clothing, with the lightest clo value equal to 0.5 for the hottest month.

Even without humidity control (see system description above), and given the dry Denver climate, both systems provided interior conditions reasonably consistent with ASHRAE Standard 55: Both had fewer than 10 operational hours within the cooling season for which the humidity ratio exceeded 0.012 kg/kg (0.012 lb/lb). This limit is equivalent to 64% relative humidity (RH) at 75°F (24°C). Both had fewer than 5 hours with RH

Table 1: Relative May through September HVAC system energy for the VAV and Radiant Cooling alternatives.

Cooling Season HVAC System Energy, May–September, Denver, CO	VAV Baseline	VAV + WSFC	Savings r.t. VAV	Radiant + DOAS	Savings r.t. VAV	Savings r.t. WSFC
Chillers (VAV only), cooling towers, and chilled water pumps (MWh)	6.41	4.51	30%	2.28	64%	49%
Hydronic system pumps and evaporative cooling spray pump (MWh)	n/a	n/a	n/a	0.37	n/a	n/a
Fans (including cooling tower fan for waterside free cooling) (MWh)	3.85	4.13	-7%	0.62	84%	85%
Boilers, natural gas (MWh)	0.36	0.36	0%	0.38	-7%	-7%
HVAC system electricity (MWh)	10.26	8.33	19%	3.27	68%	61%
Total HVAC system energy, including natural gas (MWh)	10.62	8.67	18%	3.65	66%	58%

Cooling Season HVAC System Energy

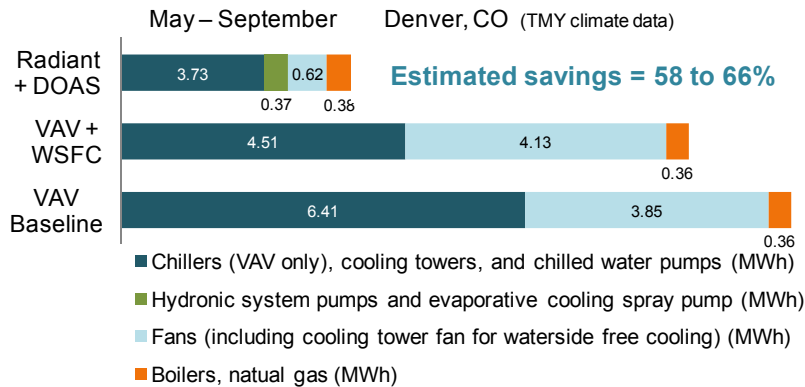


Figure 8: Comparison of simulated cooling-season HVAC system energy consumption by component.

greater than 64%, and in no instance was this coincident with peak cooling loads or space temperatures. For more humid climates, however, these systems would be set up and operated to control humidity using an appropriate cooling coil temperature reset for in the all-air VAV system and desiccant-wheel dehumidification in the case of the DOAS.

Continued development of the model and methods

While the model and methods presented here begin to get at the nuances associated with hydronic radiant cooling using a cooling tower as the chilled water source and indirect-evaporative cooling for ventilation air, there is still plenty of room for improvement in terms of both full representation of system dynamics and practical application in the design context.

Targeted future developments include refinement of four essential components of the radiant cooling and DOAS models: 1) The cooling tower models should be further developed to reflect variations in the supply water temperature range and approach to the outdoor wet-bulb temperature with changes in both the entering water temperature and outdoor wet-bulb temperatures; 2) There should be means of coupling this more complete cooling tower model directly to the hydronic cooling loop; 3) The waterside hydronic cooling model needs to permit supply water temperature and/or flow control to a slab surface temperature; 4) The dedicated outside air system would benefit from an appropriate desiccant wheel component in the airside HVAC network. The latter would permit modeling heat-driven regeneration of a desiccant wheel for dehumidification of supply air, thus extending the range of climates in which the radiant cooling system could be simulated and thus more effectively explored as a design option.

ACKNOWLEDGEMENTS

This work was made possible through the support of the California Energy Commission's Public Interest Energy Research (PIER) Program and funding from industry partners of the University of California at Berkeley Center for the Built Environment.

ABBREVIATIONS

CHW: Chilled water (vs. condenser-water loop)
COP: Coefficient of performance
DBT: Dry-bulb temperature
DOAS: Dedicated outside air system
HVAC: Heating ventilation and air-conditioning
LAT: Leaving air temperature (downstream of a coil)
OA: Outside air (as brought in by the HVAC system)
RA: Return air (from conditioned spaces)
SAT: Supply air temperature (as provided to spaces)
VAV: Variable air volume
VSD: Variable speed drive (via motor electronics)
WBT: Wet-bulb temperature
WSFC: Waterside free cooling (waterside economizer)

REFERENCES

- Alamdari, F., and G.P. Hammond. 1983. "Improved data correlations for buoyancy-driven convection in rooms." *Bldg Services Eng Research and Tech* 4(3):106–12.
- Awbi, H.B., and A. Hatton. 2000. "Mixed convection from heated room surfaces." *Energy and Bldgs* 32:153–66.
- Gough, Martin 2007. Slab conductivity adjustment tool based on Gough's 1986 solution to Laplace's equation.
- Novoselac, A., B. Burley, and J. Srebric, 2006, "New Convection Correlations for Cooled Ceiling Panels in Room with Mixed and Stratified Airflow," *HVAC&R Research*, v12, no.2